Orthogonally-Spread Block Transmissions for Ultra-Wideband Impulse Radios

Shahrokh Farahmand, Xiliang Luo, and Georgios B. Giannakis

***Abstract*—Differential, transmitted reference (TR) and energy detection (ED) based ultra-wideband impulse radios (UWB-IR) can collect the rich multipath energy offered by UWB channels with a low-complexity receiver. However, they perform satisfactorily only when the channel induced inter-pulse interference (IPI) is negligible. This can be achieved by appending a guard interval with duration greater than or equal to the channel's delay spread to each frame – an operation limiting the maximum achievable data rate. As a remedy, this Letter advocates block transmissions in conjunction with orthogonal spreading sequences to remove the introduced IPI. The resultant scheme requires no channel knowledge besides timing offset and incurs slightly more complexity than non-block alternatives, while it increases the data rate at no cost in error performance. Given a fixed data rate of 25Mbps, the novel block scheme exhibits about 1.8 dB gain relative to its non-block counterpart in single-user simulated tests.**

***Index Terms*—Differential modulation, impulse radio, transmitted reference, orthogonal code, ultra-wideband.**

I. Introduction

ULTRA-WIDEBAND impulse radios (UWB-IR) offer distinct advantages over narrowband systems, including the potential for higher data rates, simple baseband operation and ability to directly benefit from the UWB channel's rich multipath diversity. Although a RAKE receiver can be employed to collect the available multipath energy, estimation of all the tap gains and delays can be formidable as there is a large number of echoes in a typical UWB channel [8]. Furthermore, UWB-IR RAKE reception is very complex due to the large number of fingers required. Sensitivity to mistiming and channel distortions are additional challenges RAKE faces in a UWB-IR setup [17].

To alleviate RAKE limitations, the transmitted reference (TR) approach is advocated in [7] where an unmodulated reference pulse is transmitted followed by a data pulse. As both of these pulses are distorted by the same channel, the received reference pulse can be used as a correlation template to demodulate the received data pulse. TR collects all the multipath energy with much less complexity than RAKE and is more robust to mistiming, but its performance is suboptimal as the noisy template introduces a noise-noise cross-term at the autocorrelator (ACR) output that clearly degrades SNR at the decision statistic. Transmitting multiple replicas of the same pulse and pre-/post- combining them at the receiver side improves SNR [13] and will be applied in this paper's design as well. Another major limitation of TR is that reference and data pulses should be separated at least by the channel delay spread in order to avoid channel induced IPI which degrades error performance. This leads to a 50% rate loss. In addition, half of the transmitter power is wasted to send reference pulses. A differential UWB system is introduced by [6] to mitigate the 50% rate and power loss incurred by the TR system. The main idea is to use each pulse both as data as well as reference. This is achieved by differentially encoding and decoding the data. However, IPI should still be avoided to ensure acceptable performance which imposes a limit on the maximum achievable bit rate.

Rate can be increased if TR pulses are spaced increasingly closer and the resultant IPI is equalized. The ACR output in this case is well approximated by a second-order Volterra model, and several approaches have been proposed to equalize it [11], [14]. However, these algorithms require knowledge of the Volterra model parameters [11], [14], which should be estimated via periodic re-training so that a batch or adaptive equalizer can be implemented [14]. This in turn increases complexity and the associated overhead. The present Letter introduces an algorithm to increase data rate while bypassing channel estimation (Timing synchronization is needed in all options). Each data bit in the novel scheme is transmitted via several successive pulses in multiple frames. Multiple pulses allow the transceiver to maintain a certain minimum BER requirement while satisfying the spectral mask imposed by the federal communications commission (FCC) [17]. It also allows for a smaller dynamic range, thus simplifying the design of the analog frontend. In the multiuser setup, multiple pulses enable incorporation of time hopping and direct sequence codes to ensure multiple access and make the receiver robust against pulse collisions. The increased data rate of the proposed algorithm is achieved via block transmissions where multiple symbols per block are transmitted over identical frames. Each symbol in the block is further assigned a signature code orthogonal to the codes of other symbols. These orthogonal (e.g., Walsh-Hadamard) codes are employed to eliminate IPI. Consequently, rate is increased at no cost in error performance with a relatively minor increase in complexity. Under the general block transmission framework which includes TR, ED,

Manuscript received July 19, 2006; revised January 17, 2007 and November 18, 2007; accepted November 24, 2007. The associate editor coordinating the review of this paper and approving it for publication was Y. Ma. This work was supported by the NSF-ITR Grant No. EIA-0324864, NSF-MRI Grant No. CNS-0420836, and through collaborative participation in the Communications and Networks Consortium sponsored by the U. S. Army Research Laboratory under the Collaborative Technology Alliance Program, Cooperative Agreement DAAD19-01-2-0011. The U.S. Government is authorized to reproduce and distribute reprints for Government purposes notwithstanding any copyright notation thereon. Part of the results in this paper has appeared in the *Proc. of GLOBECOM Conf.*, San Francisco, CA, Nov. 27-Dec. 1, 2006.

Sh. Farahmand and G. B. Giannakis are with the Department of Electrical and Computer Engineering, University of Minnesota, 200 Union Street, Minneapolis, MN 55455, USA (e-mail: {shahrokh, georgios}@umn.edu).

X. Luo is with the Research and Development Center, Qualcomm Inc. , 5565 Morehouse Drive, San Diego, CA 92121, USA (e-mail: xl-luo@qualcomm.com).

Digital Object Identifier 10.1109/T-WC.2008.060491

and differential UWB systems, the "dual pulse technique" of [1] can be thought of as a special case of block TR system with orthogonal codes of length two namely (+1,+1) and (+1,-1). For clarity of exposition, we will consider the differential UWB system in detail. Generalizations to TR and ED are straightforward and included in the simulations.

II. Differential UWB System

Let $d(k) \in \{+1, -1\}$ denote the binary pulse amplitude modulated (PAM) data symbols to be transmitted. First, $d(k)$s are differentially encoded using the standard multiplicative recursion [6]:

$$a(k) = a(k-1)d(k-1) \qquad \forall k = 1, 2, \ldots \tag{1}$$

where $a(0) \in \{+1, -1\}$ is a fixed initial value. To guarantee a satisfactory bit error rate (BER) while respecting FCC's spectral mask and enable the application of TH and direct sequence (DS) codes for multiple access, each $a(i)$ is transmitted via N_f pulses over N_f successive frames. The transmitted signal waveform is

$$s(t) := \sqrt{\mathcal{E}_p} \sum_{k=0}^{\infty} \sum_{n=0}^{N_f-1} a(k)p(t - nT_f - kT_s) \tag{2}$$

where $\mathcal{E}_p$ is the energy per pulse, $p(t)$ is the UWB monocycle of duration T_p normalized to have unit energy, $T_f \gg T_p$ is the frame duration, and $T_s = N_f T_f$ is the symbol duration. After passing through the UWB channel and the frontend ideal low-pass filter, the received waveform is $r(t) := s(t) \star h(t) + \eta(t)$, where $\star$ denotes convolution, $h(t) := \sum_{l=0}^{L-1} \alpha_l \delta(t - \tau_l)$ represents the L-tap UWB channel and $\eta(t)$ is the low-pass filtered AWGN with two-sided power spectral density $N_0/2$. Defining[1] $g(t) := p(t) \star h(t + \tau_0)$, $r(t)$ is written as

$$r(t) = \sqrt{\mathcal{E}_p} \sum_{k=0}^{\infty} \sum_{n=0}^{N_f-1} a(k)g(t - nT_f - kT_s - \tau_0) + \eta(t). \tag{3}$$

The receiver first estimates $g(t)$ by averaging $r(t)$ over N_f frames of the kth symbol. Supposing that timing (τ_0) has been acquired (using e.g., the algorithms in [17]), the estimate of the kth symbol template $T_k(t) := a(k)g(t)$ is formed as

$$\hat{T}_k(t) = \frac{1}{N_f} \sum_{n=0}^{N_f-1} r(t + \tau_0 + nT_f + kT_s), \qquad t \in [0, T_f). \tag{4}$$

In order for $\hat{T}_k(t)$ to reliably estimate $a(k)g(t)$, IPI between successive transmissions should be negligible. The latter is possible if $T_f \geq T_p + T_d$, where $T_d := \tau_{L-1} - \tau_0$ is the channel delay spread. If T_d is not known exactly, an upper bound can be used instead. Consequently, the symbol rate will satisfy

$$R_s \leq \frac{1}{N_f T_g}, \qquad T_g := T_d + T_p. \tag{5}$$

After recovering $\hat{T}_k(t)$ as in (4), differential demodulation yields

$$\hat{d}(k-1) = \text{sign}\left[\int_0^{T_g} \hat{T}_{k-1}(t) \hat{T}_k(t) dt \right].$$

[1]The effects of UWB channel on $p(t)$ can be easily incorporated in subsequent derivations by replacing $p(t)$ with the distorted pulse $p_r(t)$ in (3), and all our conclusions will hold true in this case as well.

III. Block Differential UWB System

In this section, we will introduce our block transmission scheme which improves the data rate of the differential system in Section II. Block transmissions lead to severe IPI amongst data symbols belonging to the same frame. We will show that orthogonal spreading codes are capable of eliminating the introduced IPI. As a result, spreading can increase the rate promised by block transmissions while ensuring the same BER performance as the original system. Orthogonal codes of length two namely (+1,+1) and (+1,-1) have been used in a TR system to remove IPI between successive reference and data waveforms. In this case, the data pulse is placed arbitrarily close to the reference one to increase the data rate. This approach was advocated in [1] under the term "dual pulse technique" and can be viewed as a special case of orthogonal codes we introduce later in this section. Before beginning the exposition, recall that Walsh-Hadamard spreading codes are rows of the Hadamard matrix [10, page 424]

$$\mathbf{H}^{(1)} = \begin{bmatrix} 1 & 1 \\ 1 & -1 \end{bmatrix}, \quad \mathbf{H}^{(i)} = \begin{bmatrix} \mathbf{H}^{(i-1)} & \mathbf{H}^{(i-1)} \\ \mathbf{H}^{(i-1)} & -\mathbf{H}^{(i-1)} \end{bmatrix} \forall i \geq 2,$$

where each row is orthogonal to all others. Although any orthogonal spreading sequence can be used instead, Walsh-Hadamard ones are chosen here since they have constant modulus which is a desirable feature at the power amplification stage. Besides, Walsh-Hadamard codes entail ± 1 entries which allows for simple implementation of (de-)spreading operations in practice.

Suppose that $N_f = 2^q$, where $q \geq 0$ is a non-negative integer and select the Hadamard matrix $\mathbf{H}^{(q)}$, which yields[2] $2^q = N_f$ codes of length N_f. As for the data to be transmitted, after being differentially encoded as in (1), the symbols $a(i)$ are grouped into blocks of length N_f. Let symbol l inside block k be denoted as $a(kN_f + l)$, $l \in [0, N_f - 1]$. Instead of simply repeating $a(kN_f + l)$ over N_f frames, at the nth frame we send $a(kN_f + l)H_{l,n}$ where $H_{l,n}$ denotes the $(l+1, n+1)$th entry of $\mathbf{H}$. In other words, a Walsh-Hadamard code is used instead of the typical repetition code. All N_f symbols in a block are transmitted jointly on the same frames with delay T_p relative to each other. The transmitted waveform is given by

$$s(t) = \sqrt{\mathcal{E}_p} \sum_{k=0}^{\infty} \sum_{l=0}^{N_f-1} \sum_{n=0}^{N_f-1} a(kN_f + l)H_{l,n} \times p(t - lT_p - nT_f - kT_s). \tag{6}$$

Fig. 1 depicts transmission of a sample block with $N_f = 4$, where four symbols are to be transmitted across four successive frames resulting in a rate of one symbol per frame compared to one symbol per four frames in the original scheme. For illustration purposes, all four symbols are set to +1. The ith symbol in the jth frame is multiplied by the (i, j)th element of $\mathbf{H}^{(2)}$. Observe that summing the four frames with corresponding signs of $(+1, +1, +1, +1)$ which is the spreading code for symbol 1 eliminates the waveforms of symbols 2, 3, and 4. The same holds true for the other symbols

[2]From now on we drop the superscript for simplicity and use $\mathbf{H}$ instead of $\mathbf{H}^{(q)}$.

in the figure. In general, there are N_f distinct orthogonal codes of length N_f, so we can transmit at most N_f symbols per N_f frames leading to a data rate of one symbol per frame. After low-pass filtering and timing acquisition at the receiver, an estimate for $T_{k,l}(t) := a(kN_f + l)g(t)$ is formed as

$$\hat{T}_{k,l}(t) = \frac{1}{N_f} \sum_{n=0}^{N_f-1} H_{l,n} r(t + \tau_0 + lT_p + nT_f + kT_s) \quad (7)$$

where $t \in [0, T_g)$, $l \in [0, N_f - 1]$, and

$$r(t) = \sqrt{\mathcal{E}_p} \sum_{k=0}^{\infty} \sum_{l=0}^{N_f-1} \sum_{n=0}^{N_f-1} a(kN_f + l) H_{l,n} \times g(t - lT_p - nT_f - kT_s - \tau_0) + \eta(t) \quad (8)$$

is the received waveform. While IPI and inter-frame interference (IFI) coincide in the differential system of Section II, they are different in the block transmission format. IPI within each frame amounts to inter-symbol interference within a block and occurs among symbols with different l indices and the same k index in (8). As shown in the next section, IPI is completely removed using orthogonal codes. However, IFI can occur among symbols with different n indices in (8) and is avoided by choosing the frame length to be larger than the channel delay spread; i.e., by selecting $T_f \geq N_f T_p + T_d$. Consequently, the maximum achievable symbol rate is limited to

$$R_s \leq \frac{1}{N_f T_p + T_d}. \quad (9)$$

Given the fact that $T_p \ll T_d$, this rate increase is substantial when compared to (5). In fact, as N_f increases the improvement is more pronounced. For $N_f = 1$ no rate improvement is possible and the proposed scheme boils down to the differential UWB system of [6]. Data detection is the final step which yields

$$\hat{d}(kN_f + l - 1) = \text{sign}\left[\int_0^{T_g} \hat{T}_{k,l-1}(t)\hat{T}_{k,l}(t)dt\right], \; l \in [1, N_f - 1]. \quad (10)$$

For $l = 0$, $\hat{T}_{k,l-1}(t)$ in (10) is replaced by $\hat{T}_{k-1,N_f-1}(t)$. Note that the present block differential scheme is capable of transmitting at a symbol rate close to N_f times higher than the original system in [6]. Rate can be increased further if all the symbols in each block are transmitted simultaneously rather than with relative T_p delays. This leads to the transmitted waveform

$$s(t) = \sqrt{\mathcal{E}_p} \sum_{k=0}^{\infty} \sum_{n=0}^{N_f-1} \left(\sum_{l=0}^{N_f-1} a(kN_f + l) H_{l,n} \right) p(t - nT_f - kT_s). \quad (11)$$

To eliminate IFI in (11), one should choose $T_f \geq T_g$ leading to achievable rates as high as $R_s \leq 1/T_g$ which is higher than (9) and N_f times greater than (5). One disadvantage of simultaneous block transmission is the N_f-fold increase in peak-to-peak amplitude (a.k.a. dynamic range) compared to the delayed block transmission in (6). A waveform with large dynamic range saturates the transmitter's analog frontend and leads to waveform distortion, thus necessitating pre-distortion to reduce the peak-to-peak amplitude. For this reason, the system in (6) with delayed block transmissions is preferred although it can afford lower rate.

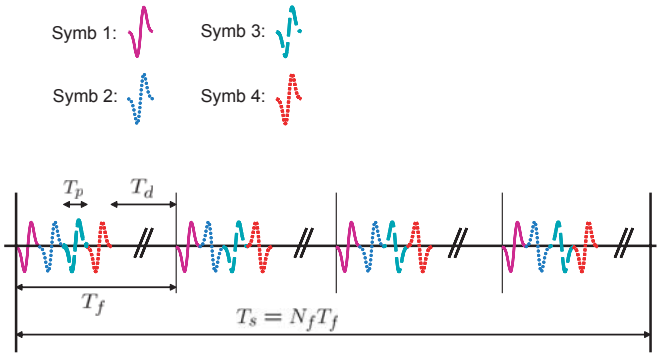

Fig. 1. An illustration of how the novel block transmission system works.

IV. Performance Analysis

We assume that the receiver has perfect timing knowledge (τ_0 is known at the receiver). Upon substituting $r(t)$ from (8) into (7), we obtain

$$\hat{T}_{k,l}(t) = \frac{1}{N_f} \sum_{n=0}^{N_f-1} H_{l,n} \left[\sqrt{\mathcal{E}_p} \sum_{k_1=0}^{\infty} \sum_{l_1=0}^{N_f-1} \sum_{n_1=0}^{N_f-1} a(k_1 N_f + l_1) \times H_{l_1,n_1} g\left(t + (l - l_1)T_p + (n - n_1)T_f + (k - k_1)T_s\right) \right] + \xi_{k,l}(t) \quad (12)$$

for $t \in [0, T_g)$, where

$$\xi_{k,l}(t) := \frac{1}{N_f} \sum_{n=0}^{N_f-1} H_{l,n} \eta(t + \tau_0 + lT_p + nT_f + kT_s), \; t \in [0, T_g) \quad (13)$$

denotes the noise contribution in $\hat{T}_{k,l}(t)$, and $\eta(t)$ is a low-pass filtered AWGN with two-sided power spectral density $N_0/2$ and low-pass filter bandwidth equal to $1/T_p$. IFI suppression which is ensured by design, forces the signal term in the right hand side of (12) to be zero except when both $n = n_1$ and $k = k_1$ are satisfied, thus yielding

$$\begin{aligned} \hat{T}_{k,l}(t) &= \frac{1}{N_f} \sum_{n=0}^{N_f-1} H_{l,n} \sqrt{\mathcal{E}_p} \sum_{l_1=0}^{N_f-1} a(kN_f + l_1) H_{l_1,n} \times g\left(t + (l - l_1)T_p\right) + \xi_{k,l}(t) \\ &= \frac{1}{N_f} \sum_{l_1=0}^{N_f-1} \sqrt{\mathcal{E}_p} a(kN_f + l_1) g\left(t + (l - l_1)T_p\right) \times \sum_{n=0}^{N_f-1} H_{l,n} H_{l_1,n} + \xi_{k,l}(t) \\ &= \sqrt{\mathcal{E}_p} a(kN_f + l) g(t) + \xi_{k,l}(t). \end{aligned} \quad (14)$$

The second equality in (14) is just a reordering of the first one while the last equality follows from the orthogonality of the spreading code:

$$\sum_{n=0}^{N_f-1} H_{l,n} H_{l_1,n} = \begin{cases} N_f, & l_1 = l \\ 0, & l_1 \neq l \end{cases} \quad (15)$$

One can observe from (14) how IPI is eliminated by the proposed orthogonal coding scheme. Plugging (14) into (10), the decision statistic can be written as

$$\hat{d}(kN_f + l - 1) = \text{sign}\left[d(kN_f + l - 1)\mathcal{E}_p \int_0^{T_g} g^2(t)dt + \zeta_1 + \zeta_2 + \zeta_3 \right],$$

where

$$\zeta_1 := \int_0^{T_g} \sqrt{\mathcal{E}_p} a(kN_f + l) g(t) \xi_{k,l-1}(t) dt,$$
$$\zeta_2 := \int_0^{T_g} \sqrt{\mathcal{E}_p} a(kN_f + l - 1) g(t) \xi_{k,l}(t) dt,$$
$$\zeta_3 := \int_0^{T_g} \xi_{k,l-1}(t) \xi_{k,l}(t) dt. \quad (16)$$

Even though these terms look similar to those encountered in the timing with dirty templates (TDT) operation in [3], [18], a subtle difference arises. Observe in (13) that the noise terms $\xi_{k,l-1}$ and $\xi_{k,l}$ that appear in ζ_3 in (16) are made up of overlapping segments of η; hence, they are correlated in general, and ζ_3 could have nonzero mean. This is not the case in TDT-based demodulator [3], where the two terms are formed from different segments of η and are uncorrelated. However, the noise terms $\xi_{k,l-1}$ and $\xi_{k,l}$ in (13) are formed by spreading the same segments of η with two different orthogonal codes. As a result, they remain uncorrelated and this allows one to apply the TDT results directly.

To make the above argument rigorous, we note that the data symbols $d(i)$, from which $a(i)$s are derived, take ± 1 values equi-probably. Hence, the transmitted symbols $a(i)$ are uncorrelated and zero-mean as well [c.f. (1)]. Using the zero-mean property of $a(i)$, it can be easily verified that ζ_1 and ζ_2 are zero-mean. Next, we prove that ζ_3 is zero-mean as well. Starting with the definition of ζ_3 in (16) and $\xi_{k,l}(t)$ in (13), we obtain

$$\begin{aligned}
\mathrm{E}[\zeta_3] &= \int_0^{T_g} \mathrm{E}\left[\xi_{k,l}(t)\xi_{k,l-1}(t)\right] dt \\
&= \int_0^{T_g} \frac{1}{N_f^2} \sum_{n_1=0}^{N_f-1} \sum_{n_2=0}^{N_f-1} H_{l,n_1} H_{l-1,n_2} \\
&\quad \times \mathrm{E}\Big[\eta(t + \tau_0 + lT_p + n_1 T_f + kT_s) \\
&\quad \times \eta(t + \tau_0 + (l-1)T_p + n_2 T_f + kT_s)\Big] dt \\
&= \frac{1}{N_f^2} \sum_{n_1=0}^{N_f-1} \sum_{n_2=0}^{N_f-1} H_{l,n_1} H_{l-1,n_2} \\
&\quad \times \int_0^{T_g} R_\eta(T_p + (n_1 - n_2)T_f) dt \quad (17)
\end{aligned}$$

where $R_\eta(\tau) := \mathrm{E}[\eta(t+\tau)\eta(t)]$ is the auto-correlation function of $\eta(t)$ given by

$$R_\eta(\tau) = \frac{N_0}{T_p} \mathrm{Sinc}\left(\frac{2\tau}{T_p}\right) = \frac{N_0 \sin(\frac{2\pi\tau}{T_p})}{2\pi\tau}$$

with $\mathrm{Sinc}(x) := \sin(\pi x)/(\pi x)$. Observing that $R_\eta(\tau) \approx 0$ for $\tau \gg T_p$ and using the fact that $T_f \gg T_p$, we deduce that $R_\eta(T_p + (n_1 - n_2)T_f)$ is nonzero only when $n_1 = n_2$. So (17) is further written as

$$\begin{aligned}
\mathrm{E}[\zeta_3] &= \frac{1}{N_f^2} \sum_{n_1=0}^{N_f-1} H_{l,n_1} H_{l-1,n_1} \int_0^{T_g} R_\eta(T_p) dt \\
&= \frac{1}{N_f^2} R_\eta(T_p) T_g \sum_{n_1=0}^{N_f-1} H_{l,n_1} H_{l-1,n_1} = 0
\end{aligned}$$

where the last equality follows due to the code orthogonality in (15).

Power calculations for $\zeta_1, \zeta_2, \zeta_3$ are similar to their TDT counterparts that have been carried out in [3], [18] and the references thereon, yielding

$$\mathrm{E}[\zeta_1^2] = \mathrm{E}[\zeta_2^2] = \frac{\mathcal{E}_p N_0}{2N_f}, \qquad \mathrm{E}[\zeta_3^2] = \frac{1}{2}\left(\frac{N_0}{N_f}\right)^2 \left(\frac{T_g}{T_p}\right)$$

where a normalized UWB channel is assumed so $\int_0^{T_g} g^2(t)dt = 1$. We also note that ζ_1, ζ_2, and ζ_3 are mutually uncorrelated due to the zero-mean property of $a(i)$s. As a result, the received SNR is found as

$$\mathrm{SNR} = \left[\frac{N_0}{\mathcal{E}_p N_f} + \frac{1}{2}\left(\frac{N_0}{\mathcal{E}_p N_f}\right)^2 \left(\frac{T_g}{T_p}\right)\right]^{-1}. \quad (18)$$

Both ζ_1 and ζ_2 are Gaussian while ζ_3 can be approximated as Gaussian [16, Appendix I]. Hence, for binary PAM the probability of error is given by $P_e \approx Q(\sqrt{\mathrm{SNR}})$, where $Q(x) := (1/\sqrt{2\pi}) \int_x^\infty e^{-t^2/2} dt$. A similar calculation for the differential UWB radio of Section II, leads to the same SNR as in (18) proving that no performance is lost by block transmissions. However, the receiver now needs more adders and multipliers and $N_f - 1$ additional delay lines to shift the received waveform by multiples of T_p which is the price paid for the higher data rate. The following remark addresses pertinent implementation issues.

Remark 1: The proposed block differential systems can be implemented either in analog or in digital fashion. The delay elements can be implemented with available analog delay lines [2], although digital implementations are usually preferred since they exhibit improved reliability [4]. As for the digital implementation, if Nyquist rate sampling (2 GHz for $T_p = 1$ nsec) can be afforded, the averaging and integration operations in (7) and (10) can be performed digitally using the sampled waveforms. As sampling at these high rates is challenging, sub-Nyquist rate sampling can be considered for easier implementation at the cost of error performance degradation [5].

V. Simulations

The LOS Channel model 1 in [8] is used in the simulations and $T_d = 34$ nsec is chosen to capture most of the UWB multipath channel. The UWB monocycle pulse is selected as the second derivative of the Gaussian pulse in [3] with duration $T_p = 1$ nsec. The first simulation compares the differential UWB system of Section II with its counterpart in Section III for a single-user set up. We have chosen $N_f = 4$, and $T_f = 40$ nsec for the block differential detector and $T_f = 10$ nsec for the original differential system. The bit-rate is $1/T_f$ for the block differential system and $1/N_f T_f$ for the original differential system, leading to the same rate of 25 Mbps for both schemes. This choice of parameters effects severe IPI to both receivers, and helps illuminate the advantages gained by using IPI eliminating codes in the block transmission scheme. TR and ED-based receiver and their counterparts with block transmissions are considered as well. The data rate for all the systems is fixed at 25 Mbps. One in each N_f symbols is used as a reference in TR, i.e., the frame

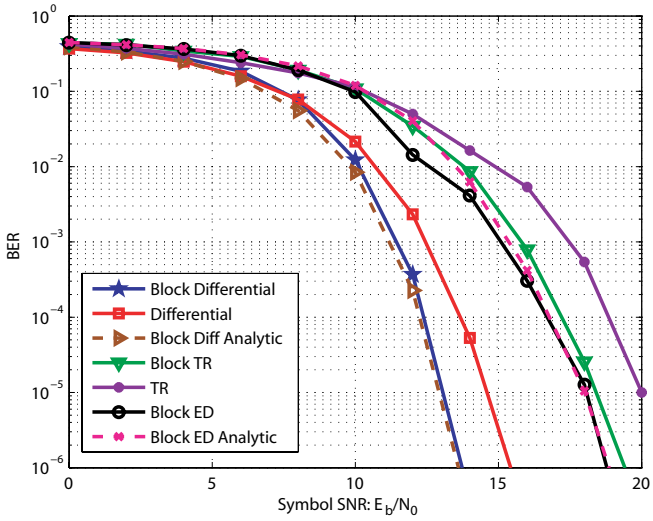

Fig. 2. BER comparison of single user block differential and TR with their non-blocked versions in Section II.

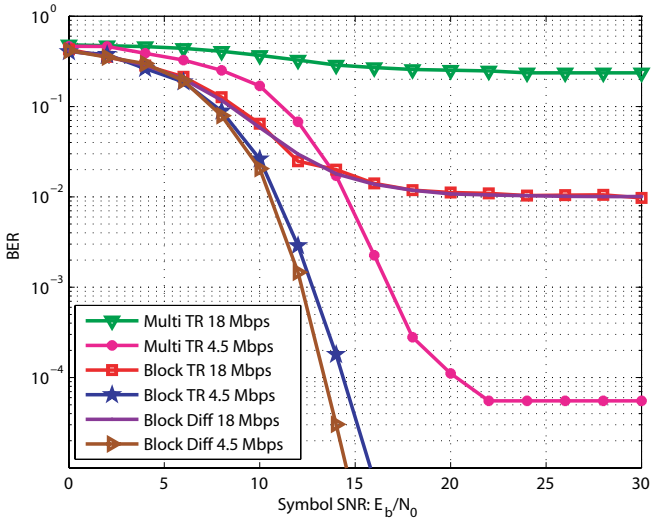

Fig. 3. BER comparison of block differential and TR systems with the multiuser TR of [15].

length is scaled so that the same data rate as the differential system is achieved. The ED-based receiver in [9] with an on-off keying (OOK) modulation is considered where the optimal threshold is chosen according to the Gaussian approximation rule of [12]. Fig. 2 plots BER versus symbol SNR ($\mathcal{E}_b/N_0$) where $\mathcal{E}_b := N_f\mathcal{E}_p$. The averaging window size is fixed to 4 frames (one symbol duration) for all schemes. It is observed that the difference between differential and block differential schemes becomes more pronounced as SNR increases (for BER equal to 10^{-5}, the SNR gap is 1.8 dB). This is expected as in the high SNR regime noise effects are negligible and IPI is the major limiting factor. The BER evaluated analytically in Section IV is also plotted. In Fig. 2, we observe a considerable gap (about 5 dB) between block differential and block TR systems. This is partly due to the effect of frame scaling for TR. To attain the same rate as the block differential system, block TR needs a frame length of $T_f = 30$ nsec which causes residual IFI and deteriorates error performance. The second reason for this sizeable gap is power scaling. Since the TR system uses $N_f = 4$, about 1.25 dB of each symbol's energy is used to send pilots. The rest of the 5 dB gap (3.75 dB) is attributed to the residual IFI as mentioned above. Simulated BER for block ED is also plotted. For this data rate, the non-block ED is not operational since severe IPI renders reliable demodulation impossible.

The second simulation considers a multiuser setup where random DS and TH codes are incorporated to enable multiple access. Simulated BER for the downlink multiuser TR proposed by [15] is plotted for comparison. The multiuser TR of [15] is chosen because it addresses the same ISI issue. However, it removes ISI by using random codes rather than deterministic ones. It does so by first estimating and then subtracting the reference pulse from the received waveform, thus removing its ISI effect from the data waveform. For the multiuser differential system, we choose $N_f = 16$ and $T_f = 56$ nsec. If we were to take full advantage of block transmissions, we should transmit 16 symbols over 16 frames to attain a bit-rate of 18 Mbps. In this case, a TH code of length 6 should be employed. However, we might be willing to trade-off data rate for performance and transmit 4 symbols every 16 frames while keeping T_f constant resulting in a bit rate of 4.5 Mbps with a TH code of length 18. The same bit rates for the multiuser TR system requires frame length $T_f = 14$ nsec for 4.5 Mbps and $T_f = 4$ nsec for 18 Mbps. Given these choices, the BER for the two schemes is plotted versus symbol SNR in Fig. 3. The averaging window size is fixed to 16 frames (one symbol duration) for both schemes. There are 3 interferers with the same SNR as the desired user. The block differential system clearly outperforms the multiuser TR for the same rate and averaging window size. This is expected as the IPI eliminating pseudo-random codes of multiuser TR need large window sizes to effectively remove IPI, while the deterministic codes of the block differential detector eliminate IPI with an averaging window size of one symbol. As for the differential detector, rate reduction from 18 to 4.5 Mbps pays off well since the gained performance is indeed considerable. The BER curves corresponding to the block TR system are also plotted. As expected, its performance is inferior to the multiuser block differential system while it is superior to the multiuser TR system in [15].

VI. Conclusions

The IPI in differential, TR, and noncoherent (i.e., ED based) UWB radios severely degrades bit error performance. If frame length is restricted to be greater than the channel delay spread to avoid IPI, the maximum achievable rate is limited. This paper introduced a block transmission format to increase the data rate of UWB-IR systems. Block transmissions however, lead to severe IPI which necessitated orthogonal Walsh-Hadamard spreading codes to eliminate the introduced IPI. Analytical derivations for a point-to-point UWB link proved that the improved rate of block transmissions is achieved at no cost in BER performance. Simulations for single-user and multiuser scenarios were carried out for fixed data rates and fixed number of transmitted pulses per symbol. It was observed that the novel block transmission technique improved the

BER performance of differential, TR and ED-based receivers compared to their non-block counterparts. [3]

REFERENCES

[1] X. Dong, A. C. Y. Lee, and L. Xiao, "A new UWB dual pulse transmission and detection technique," in *Proc. ICC*, pp. 2835-2839, Seoul, Korea, May 2005.

[2] ELMEC Technology [Online].
Available: http://www.elmectech.com/elmec/elmec_ home.html.
Data Sheet: http://www.elmectech.com/cdm/cdm_ all.html.

[3] Sh. Farahmand, X. Luo, and G. B. Giannakis, "Demodulation and tracking with dirty templates for UWB impulse radio: algorithms and performance," *IEEE Trans. Veh. Technol.*, vol. 54, no. 5, pp. 1595-1608, Sept. 2005.

[4] S. Franz and U. Mitra, "Generalized UWB transmitted reference systems," *IEEE J. Select. Areas Commun.*, vol. 24, no. 4, pp. 780-786, Apr. 2006.

[5] I. Guvenc and H. Arslan, "Bit error rates of IR-UWB transceiver types at sub-Nyquist sampling rates," in *Proc. IEEE Wireless Communication and Networking Conference (WCNC)*, Las Vegas, NV, Apr. 2006.

[6] M. Ho, V. S. Somayazulu, J. Foerster, and S. Roy, "A differential detector for an ultra-wideband communication system," in *Proc. Vehicular Technology Conf.*, pp. 1896-1900, Birmingham, AL, May 2002.

[7] R. Hoctor and H. Tomlinson, "Delay-hopped transmitted-reference RF communications," in *Proc. Conf. on UWB Systems and Technologies*, pp. 265-269, Baltimore, MD, May 2002.

[8] IEEE P802.15 Working Group for WPANs, *Channel Modeling Sub-Committee Report Final*, IEEE P802.15-02/368r5-SG3a, Nov. 2002.

[9] S. Paquelet, L.-M. Aubert, and B. Uguen, "An impulse radio asynchronous transceiver for high data rates," in *Proc. IEEE Ultra-wideband Syst. Technology (UWBST)*, pp. 1-5, Kyoto, Japan, May 2004.

[10] J. G. Proakis, *Digital Communications*. McGraw-Hill, fourth edition, 2000.

[11] J. Romme and K. Witrisal, "Transmitted-reference UWB systems using weighted autocorrelation receivers," *IEEE Trans. Microwave Theory and Techniques*, vol. 54, no. 5, pp. 1754-1761, Apr. 2006.

[12] M. E. Sahin, I. Guvenc, and H. Arslan, "Optimization of energy detector receivers for UWB systems," in *Proc. IEEE Vehicular Technology Conference*, pp. 1386-1390, Stockholm, Sweden, May 2005.

[13] F. Tufvesson and A. F. Molisch, "Ultra-wideband communication using hybrid matched filter correlation receivers," *Proc. Vehicular Technology Conference*, Los Angeles, CA, pp. 3511-3516, May 2004.

[14] K. Witrisal, G. Leus, M. Pausini, and C. Krall, "Equivalent system model and equalization of differential impulse radio UWB systems," *IEEE J. Select. Areas Commun.*, vol. 23, no. 9, Sept. 2005.

[15] Z. Xu and B. M. Sadler, "Code aided near full rate multiuser TR-UWB systems," in *Proc. SPAWC*, pp. 980-984, New York, NY, June 2005.

[16] L. Yang and G. B. Giannakis, "Optimal pilot waveform assisted modulation for ultrawideband communications," *IEEE Trans. Wireless Commun.*, vol. 3, no. 4, pp. 1236-1249, July 2004.

[17] L. Yang and G. B. Giannakis, "Ultra-wideband communications: an idea whose time has come," *IEEE Signal Processing Mag.*, vol. 21, no. 6, pp. 26-54, Nov. 2004.

[18] L. Yang and G. B. Giannakis, "Timing ultra-wideband signals with dirty templates," *IEEE Trans. Commun.*, vol. 53, no. 11, pp. 1952-1963, Nov. 2005.

[3]The views and conclusions contained in this document are those of the authors and should not be interpreted as representing the official policies, either expressed or implied, of the Army Research Laboratory or the U. S. Government.